YALE PEABODY MUSEUM

JOURNAL OF MARINE RESEARCH

The *Journal of Marine Research,* one of the oldest journals in American marine science, published important peer-reviewed original research on a broad array of topics in physical, biological, and chemical oceanography vital to the academic oceanographic community in the long and rich tradition of the Sears Foundation for Marine Research at Yale University.

An archive of all issues from 1937 to 2021 (Volume 1–79) are available through EliScholar, a digital platform for scholarly publishing provided by Yale University Library at https://elischolar.library.yale.edu/.

Requests for permission to clear rights for use of this content should be directed to the authors, their estates, or other representatives. The *Journal of Marine Research* has no contact information beyond the affiliations listed in the published articles. We ask that you provide attribution to the *Journal of Marine Research.*

Yale University provides access to these materials for educational and research purposes only. Copyright or other proprietary rights to content contained in this document may be held by individuals or entities other than, or in addition to, Yale University. You are solely responsible for determining the ownership of the copyright, and for obtaining permission for your intended use. Yale University makes no warranty that your distribution, reproduction, or other use of these materials will not infringe the rights of third parties.

Influence of advective bio-irrigation on carbon and nitrogen cycling in sandy sediments

by Taehee Na[1,2], Britta Gribsholt[3,4], Oleksiy S. Galaktionov[3], Tongsup Lee[1] and Filip J. R. Meysman[3,5]

ABSTRACT

In sandy sediments, the burrow ventilation activity of benthic macrofauna can generate substantial advective flows within the sediment surrounding their burrows. Here we investigated the effects of such advective bio-irrigation on carbon and nitrogen cycling in sandy sediments. To this end, we combined a range of complementary experimental and modelling approaches in a microcosm study of the lugworm *Arenicola marina* (Polychaeta: Annelida). Bio-irrigation rates were determined using uranine as a tracer, while benthic fluxes of oxygen (O_2), total carbon dioxide (TCO_2), dissolved inorganic nitrogen (NH_4^+, $\Sigma NO_2^- + NO_3^-$) and dinitrogen (N_2) were measured in closed-core incubations containing lugworms acclimatized for a relatively short (2 d) and long (3 wk) duration. The fluxes induced by *A. marina* were compared to those induced by mechanical mimics that simulate the flow pattern induced by the lugworm. These mechanical mimics proved a useful tool to simulate the effect of lugworm irrigation on sediment biogeochemistry. Subsequently, reactive transport model simulations were performed to check the consistency of the measured fluxes and rates, and to construct closed mass balances for sedimentary nitrogen. This reactive transport model successfully captured the essential features of the nitrogen cycling within the sediment. Advective irrigation by both lugworm and mechanical mimics significantly stimulated the sediments O_2 consumption, organic matter mineralization rate (TCO_2 release), and denitrification rate (N_2 production). While sedimentary O_2 consumption was directly correlated to advective input of O_2, increasing irrigation rates increased the importance of coupled nitrification-denitrification over the external input of nitrate from the overlying water.

1. Introduction

Coastal sediments are inhabited by macrofauna that create burrows or burrow networks that penetrate deeply into the anoxic zone of the sediment (Rhoads, 1974). These burrows are flushed with oxygen-rich water from the overlying water column, and this process of

1. Division of Earth Environmental System, Pusan National University, Busan 609 735, Korea.
2. Corresponding author. *email: ocean95@pusan.ac.kr*
3. Netherlands Institute of Ecology, Centre for Estuarine and Marine Ecology, P. O. Box 140, 4400 AC Yerseke, The Netherlands.
4. Department of Biological Sciences, Center for Geomicrobiology, University of Aarhus, Building 1540, Ny Munkegade, DK-8000 Aarhus C, Denmark.
5. Department of Analytical and Environmental Chemistry, Vrije Universiteit Brussel (VUB), Pleinlaan 2, B-1050 Brussel, Belgium.

bio-irrigation serves a number of ecological purposes, including oxygen supply, metabolite removal and/or filter-feeding (Aller, 2001). Bio-irrigation exerts a strong influence on various aspects of the biogeochemistry of coastal sediments, for instance on organic matter processing (e.g., Aller and Aller, 1998; Kristensen, 2001; D'Andrea *et al.,* 2002), N-cycling (e.g., Kristensen *et al.,* 1991; Gilbert *et al.,* 2003), microbial ecology (e.g., Reichardt, 1988; Marinelli *et al.,* 2002), and solute exchange with the overlying water (e.g., Huettel, 1990; Meile and Van Capellen, 2003).

Despite the many insights gained in previous studies, our knowledge about the exact biogeochemical role of bio-irrigation remains surprisingly qualitative, and hence, accurate quantitative predictions remain difficult to achieve. Based on past experience, we can foretell that bio-irrigating macrofauna will substantially alter solute fluxes and biogeochemical rates within the sediment (e.g., Pelegri and Blackburn, 1994; Webb and Eyre, 2004), but exactly how much these fluxes and rates will increase, and why they increase the way they do, remain largely unresolved. Therefore, improving our quantitative and mechanistic understanding of bio-irrigation remains a true challenge. This is particularly true for sandy sediments. Given that sandy sediments make up a substantial fraction of shelf sediments (Emery, 1966), an accurate assessment of the biogeochemical influence of advective bio-irrigation is vital for our understanding of carbon and nitrogen cycling in such sediments.

Due to the higher permeability, advective flow of pore water dominates solute transport in sandy environments (e.g. Reimers *et al.,* 2004). The pressure gradients that drive advective pore flow in sandy sediments can be classified as either being physical or biological in origin (Meysman *et al.,* 2007). Physically driven pore water flow results from wave action (Riedl *et al.,* 1972; Precht and Huettel, 2003) or from bottom currents interacting with sediment topography, such as sand ripples induced by currents (e.g. Thibodeaux and Boyle, 1987; Cardenas and Wilson, 2007), or the pits and mounds created by benthic organisms (Huettel and Gust, 1992; Ziebis *et al.,* 1996). The biogeochemical effects of both wave-driven and topography-driven advection have recently received considerable attention, both *in situ* (De Beer *et al.,* 2005; Janssen *et al.,* 2005), as well as in detailed process studies under laboratory conditions (e.g. Franke *et al.,* 2006; Rao *et al.,* 2007, 2008).

Yet, pore water flow may also be directly induced by burrowing organisms, and this mechanism may be the dominant control on solute exchange in coastal sandflats with high abundances of bio-irrigators. When ventilating their burrows, organisms are able to generate flow within the sediment surrounding the burrow (Huettel, 1990; Walbusser and Marinelli, 2006; Meysman *et al.,* 2006). This advective mechanism of bio-irrigation has been hypothesized to be more efficient than the radial diffusion of solutes from the burrow, which characterizes bio-irrigation in muddy sediments (Riisgård and Banta, 1998; Kristensen, 2001). In addition, the spatial configuration and depth dependency of biologically-induced advection is very different from that of physically-induced advection. The effects of waves and topography are most intense near the sediment-water interface and diminish

with depth, thus mostly affect the first 5–10 cm of the sediment (Shum and Sundby, 1996; Huettel *et al.,* 1996). In contrast, bio-irrigation does not need to follow such a regular depth dependency. Burrows can extend far down into the sediment (e.g. tens of centimetres in the case of lugworms and up to meters in the case of thallianassid shrimp), and so intense advective currents can be generated at substantial depth into the anoxic zone.

Here we focus on the biologically induced advection in driving biogeochemistry in permeable sandy sediments. For this purpose, we present a case study of the lugworm *Arenicola marina* (Polychaeta: Annelida). Lugworms are abundant in coastal sandy areas worldwide, and are dominant bio-irrigators in these systems (Riisgård and Banta, 1998). They are head-down deposit feeders that live at 20 to 40 cm depth in a J-shaped burrow. They inject burrow water at depth, which causes an upward percolation of pore water and seepage across the sediment-water interface (Meysman *et al.,* 2005). Our main aim is to investigate how advective bio-irrigation affects the C and N cycles in permeable sandy sediments. Because of their strong irrigation activity, lugworms have been used before in studies of advective bio-irrigation (Banta *et al.,* 1999; Papaspyrou *et al.,* 2007). However, these studies were typically limited to flux rate measurements and down-core concentration profiles of solutes and solids. Here we employ three additional techniques that complement these experimental methods. (1) Using the uranine tracer method (Meysman *et al.,* 2007), we quantify the bio-irrigation rate separately and independently from the biogeochemical fluxes and rates (O_2 consumption, denitrification, nutrient fluxes). (2) We compare the biogeochemical effects of actual lugworms with those of mechanical mimics that simulate the flow pattern induced by lugworm irrigation. (3) Using a previously developed reactive transport model of the sediment surrounding lugworm burrows (Meysman *et al.,* 2006, 2007), we perform model simulations that allow us to check the consistency of independently measured fluxes and rates, and from which we can derive closed mass balances for sedimentary nitrogen.

2. Materials and methods

a. Experimental set-up

Sandy sediment (median grain size 200 μm) was obtained from a tidal flat of the Oosterschelde (south-western Netherlands) in July 2006. The lugworm *A. marina* is the dominant macrofaunal species on this tidal flat, with densities ranging up to 50 ind. m^{-2}. Lugworm specimen were collected from the same location as the sediment and selected within a certain size class (8.6 ± 1.1 g wet weight). Lugworms were added to the incubation cores immediately after collection.

Twelve Plexiglas cores (50 cm long, 10.2 cm internal diameter) were filled with approximately 20 cm of sediment. The sediment was first sieved through a 0.5 mm mesh to remove macrofauna and large particles, and homogenized by hand. Cores were placed submerged in an incubation tank containing ambient sea water (~400 L). The tank was well aerated, placed in a temperature controlled room (20°C) in darkness, and the water

was changed twice a week. The water overlying each sediment core was continuously stirred by two Teflon coated magnets. The rate at which the water was stirred in each core was kept well below the resuspension limit (<30 rpm).

Twelve cores were used in total, divided over four different treatments with triplicate cores. Treatments are referred to as "fresh worms", "acclimated worms", "mimics" and "control". In all treatments, the sediment cores were allowed to "equilibrate" for 25 days before the start of the incubations to allow the development of geochemical "steady-state" conditions. The "fresh worm" and "acclimated worm" treatments both involved the addition of similar lugworms, but the organisms were added at different times, resulting in distinct "acclimation" periods. In the "acclimated worm" treatment lugworms were added at day 3 of the experiment (i.e., 22 days before the start of incubations), while in the "fresh worm" treatment lugworms were added at day 23 of the experiment (i.e., only 2 days prior to the start of incubations). The aim was to investigate how strongly the acclimation under artificial laboratory conditions would influence lugworm bio-irrigation activity, and hence, the fluxes measured during incubations. Negative effects on organism activity may result from the prolonged removal from the natural environment as well as specific limitations of the experimental procedure (e.g. relatively small cores, no food addition).

The "mimic" treatment involved a mechanical pump system that served as a mechanical mimic for the bio-irrigational pore flow induced by the lugworm. Each mechanical mimic consisted of a peristaltic pump, connected via impermeable tygon® tubing (<50 cm length, 0.375 cm inner diameter) to a porous bubbling stone (2 cm diameter). The inlet tube of the peristaltic pump takes in overlying water, and pumps this via the outlet tube to the bubbling stone, which is buried centrally in the sediment core (Fig. 1b). This bubble stone represents the lugworm's feeding pocket, which is the location where burrow water is pumped into the sediment under natural conditions (Riisgård and Banta, 1998). The pumping rate of the peristaltic pump was measured at the conclusion of the experiment by placing the inlet tube in an external graduated cylinder and measuring the volume decrease over time. Mechanical mimics were left continuously pumping for 25 days prior to incubation to establish a steady-state regime. Finally, no irrigation effect (either real or artificial) was imposed in the "control" treatment, and so the sediment was left as such for 25 days prior to incubation.

b. Core sectioning and sediment parameters

After the 25 day equilibration period, various incubations and flux measurements were made over a period of 3 days (see details below). At the termination of the experiment (day 28), all cores were vertically split into two halves and photographed to visually determine the extent of oxic zone (Fig. 2). Subsequently, these core halves were horizontally sectioned into the depth intervals 0–1, 1–2, and 2–4 cm. The sediment parameters were determined for each of these subsections, and compared to the homogenous sediment that served as the starting material. The porosity ϕ was calculated from weight loss after drying at 105°C overnight. Subsamples of dried sediment were used for determination of
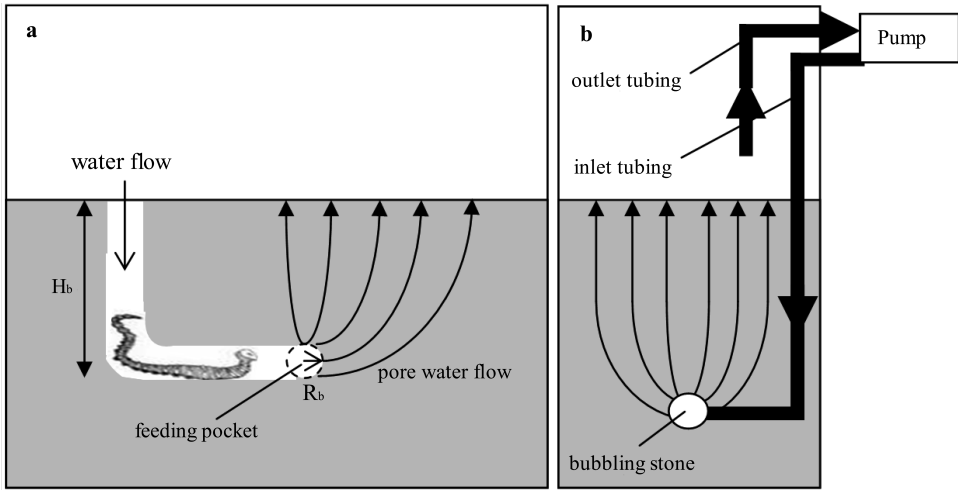
Figure 1. (a) Idealized scheme of advective bio-irrigation by the lugworm *Arenicola marina* (modified from Meysman *et al.,* 2006). The lugworm creates a J-shaped burrow (burrow depth H_b). Overlying water is pumped through the burrow and injected into the sediment across the walls of the feeding pocket (burrow radius R_b). This creates an upward water flow in the sediment. (b) Mechanical mimic of lugworm bio-irrigation. Overlying water is pumped by a peristaltic pump into the sediment via impermeable tubing and a bubbling stone, in order to mimic the flow pattern induced by the lugworm.

particulate organic carbon (POC) and nitrogen (PON) on a Carlo Erba NA 1500 elemental analyzer (Nieuwenhuize *et al.,* 1994). The solid sediment density ρ_S was measured by adding a known mass of dried sediment to a graduated cylinder, and determining the volume change.

c. Benthic flux measurements

The total oxygen uptake (TOU) and the flux across the sediment-water interface of total CO_2 ($TCO_2 = H_2CO_3 + HCO_3^- + CO_3^{2-}$), dissolved inorganic nitrogen (DIN = NH_4^+ + $NO_2^- + NO_3^-$) and dinitrogen gas (N_2) were determined on day 25. All equipment used for the incubations (lids, Teflon tubings, Luer stopcocks) were placed submerged in the incubation tank 48h prior to measurements, in order to avoid introduction of new surfaces for O_2, N_2 and Ar adsorption. This is pivotal for the correct determination of N_2 production (see below) (Kana *et al.,* 1994). Each core was sealed with an air-tight lid and incubated for 8–10 h in darkness. Incubation time depended on the change in oxygen concentration, which was never allowed to decrease below 50% air-saturation.

All samples were drawn from the overlying water via Luer stopcock sample ports with a gas-tight glass syringe. Refill water was allowed to enter via separate Luer stopcocks from the tank water surrounding the cores. Samples for TCO_2 and O_2 were only collected at the start and end of core incubation, while those for the determination of N_2 and dissolved

a. control   b. fresh lugworm   c. mechanical mimic
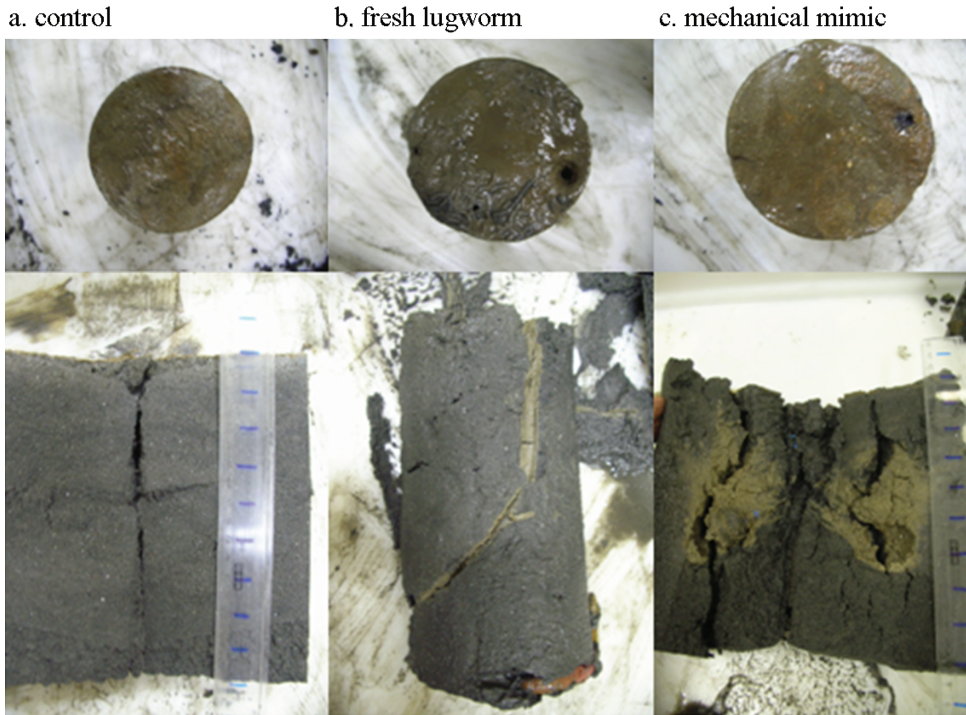

Figure 2. Photographs of the sediment surface (upper panel) and a vertical cross section through the middle plane of the cores (lower panel) for the different treatments. In the lower panel of (b) the lugworm is visible at the bottom right. Note that panel (b) only shows one half of the split core, while panels (a) and (c) show the two halves side by side.

inorganic nitrogen (DIN) were collected 5 times during the incubation. For N_2 determination 10 ml Pyrex glass test tubes (in triplicate) were filled to overflow, preserved with 20 μl $HgCl_2$, capped with no headspace and stored submerged at ambient temperature. The concentration of N_2 and Ar was determined by membrane-inlet mass spectrometry (MIMS) using an Omnistar QMS 200 quadropole mass spectrometer (Baltzers Instruments, Liechtenstein) for detection (see Andersson, 2007 for details). N_2 concentrations were normalised to that of Ar (Kana *et al.,* 1994) and the N_2 production calculated from the linear increase in Ar-normalised N_2 concentration, corrected for the refill water. DIN samples were filtered through pre-combusted Whatman CF/F filters (25 mm), frozen immediately, and analyzed within 1 week using automated colorimetric techniques. Oxygen was analyzed within 24 h using standard Winkler titration (Parson *et al.,* 1984), while TCO_2 was determined using the flow injection/diffusion cell technique of Hall and Aller (1992). O_2 and TCO_2 fluxes were calculated from the concentration difference between initial and final samples, assuming constant solute exchange with time, and compensating for the dilution by refill water.

d. Bio-irrigation rate measurements

The bio-irrigation rate represents the volumetric exchange of water (in ml min^{-1}) between the overlying water and the pore water. Bio-irrigation rates were immediately measured after the flux incubations (day 27 of experiment). Uranine (sodium fluorescein, $C_{20}H_{10}Na_2O_5$) was used as a transport tracer to quantify this bio-irrigation rate following the method of Meysman *et al.* (2007). The overlying water of a sediment core was spiked with 4 ml of uranine stock solution (500 µg L^{-1}) and the subsequent concentration decrease in the overlying water was followed over time. A 1 ml sample was taken every ~3 hours over a period of 36 hours. Fluorescence was measured at 520 nm using a Turner Quantech Digital Fluorometer (FM 109530-33) with 490 nm as the excitation wavelength.

In Meysman *et al.* (2007) the resulting tracer data were fitted with a complex numerical model of lugworm bio-irrigation, and this model explicitly describes the flow pattern within the sediment. Here, we propose an alternative approach to arrive at the bio-irrigation rate, based on a simplified analytical solution to the governing equations (the model of Meysman *et al.,* 2007 is still used for the biogeochemical simulations—see below). The balance equations for the tracer concentrations in the overlying water (OW), the pore water (PW) and the solid sediment (S) are respectively given by

$$V_{OW} \frac{\partial C_{OW}}{\partial t} = -Q(C_{OW} - C_{PW}) \tag{1}$$

$$V_{PW} \frac{\partial C_{PW}}{\partial t} = Q(C_{OW} - C_{PW}) - R_{ad} \tag{2}$$

$$M_S \frac{\partial C_S}{\partial t} = R_{ad} \tag{3}$$

In these equations, C_{OW} and C_{PW} denote the uranine concentrations (ng ml^{-1}) in the overlying water and pore water, and C_S denotes the adsorbed uranine onto the sediment matrix (ng per g of dry sediment). The parameters V_{OW} and V_{PW} denote the volume of overlying water and pore water (ml), M_S is the mass of dry sediment (g), and Q is the exchange rate of water between water column and sediment (ml min^{-1}). The quantity R_{ad} represents the total adsorption rate of uranine onto the sediment (ng min^{-1}). If one assumes that this adsorption process is fast, one can adopt the local equilibrium relation $C_S = K_{ad}C_{PW}$, where K_{ad} is the adsorption coefficient of uranine (ml g^{-1}). Initially (that is immediately after spiking), the initial concentration of uranine in the overlying water becomes C_{OW}^0, and there is no uranine present in the sediment ($C_{PW}^0 = C_S^0 = 0$). Under these conditions, the equation set (1)–(3) allows the simple analytical solution

$$C_{OW}(t) = \frac{A}{B} C_{OW}^o + \left(1 - \frac{A}{B}\right) C_{OW}^0 \exp(-Bt) \tag{4}$$

which predicts an exponential decline of the tracer concentration over time. The parameters A and B are combinations of previously introduced quantities

$$A = \frac{Q}{V_{PW} + M_S K_{ad}}, \quad B = \frac{Q}{V_{OW}} \left(1 + \frac{V_{OW}}{V_{PW} + M_S K_{ad}} \right) \tag{5}$$

Apart from the bio-irrigation rate Q, each parameter in Eqs. (4) and (5) is constrained by actual measurements. The volume of overlying water is determined from $V_{OW} = \pi R_C^2 H_{OW}$, by measuring the core radius R_C and the height of the overlying water H_{OW}. The volume of pore water becomes $V_{OW} = \phi \pi R_C^2 H_S$, where ϕ is the porosity and H_S is the measured sediment height. Similarly, the sediment mass M_S is calculated using the relationship $M_S = \rho_S (1 - \phi) \pi R_C^2 H_S$, where ρ_S is the measured solid sediment density. Finally, the adsorption constant K_{ad} was determined from a series of batch experiments with uranine adsorption, resulting in a value of 0.80 cm^3 ml per g of dry sediment. This implies all parameters in Eq. (4) are known except for the bio-irrigation rate Q. Accordingly, by fitting Eq. (4) to the data from an uranine incubation experiment, one can estimate the bio-irrigation rate Q. The best estimate for Q was obtained by minimizing the sum of squared errors between model predictions and data points for each of the profiles (this was done using the Solver routine in Excel).
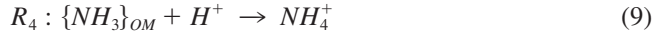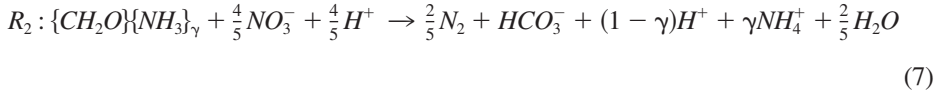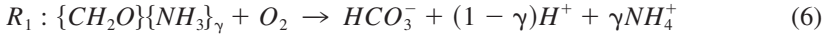
e. Biogeochemical model simulations

Numerical model simulations were performed to analyse the experimental results and to evaluate the effect of the advective bio-irrigation on oxygen consumption and denitrification. To this end, the bio-irrigation model of Meysman *et al.* (2006) was extended with a biogeochemical module. Cook *et al.* (2006) explored a similar model approach to investigate N-cycling in permeable sediments exposed to physically driven pore flow. The model output consists of concentration patterns within the sediment and biogeochemical rates associated with N-cycling (reaction rates, fluxes to the overlying water).

The bio-irrigation model is detailed in Meysman *et al.* (2006), and only a brief overview is given here. The model basically provides a mathematical description of the mechanical mimic in Figure 1b (which in itself comprises a physical analogue of real lugworm bio-irrigation). The model domain represents the sediment inside a cylindrical incubation chamber (of radius R_c), where water is pumped (with rate Q) across the walls of a spherical pocket (located at depth H_b and with radius R_b). Sediment parameters like porosity and permeability are assumed homogeneous, and the sediment surface is considered to be flat. Under such conditions, flow and concentration patterns can be described by a radially symmetric 2D model, which consists of two parts (Meysman *et al.,* 2006, 2007). A Flow Model (FM) first simulates the flow pattern within the sediment, and the resulting pore water velocity is subsequently incorporated into a Reactive Transport Model (RTM), which simulates the concentration patterns of selected components. The details of the model formulation for both FM and RTM can be found in Meysman *et al.* (2006, 2007).

In Meysman *et al.* (2006, 2007), model simulations were performed for inert tracers. Here, we extend the bio-irrigation model with a biogeochemical module that describes

N-cycling, using the reaction set of Cook *et al.* (2006). Four microbial pathways are incorporated: aerobic respiration (R_1), denitrification (R_2), nitrification (R_3), and ammonification (R_4)

$$R_1 : \{CH_2O\}\{NH_3\}_\gamma + O_2 \rightarrow HCO_3^- + (1-\gamma)H^+ + \gamma NH_4^+ \tag{6}$$

$$R_2 : \{CH_2O\}\{NH_3\}_\gamma + \tfrac{4}{5}NO_3^- + \tfrac{4}{5}H^+ \rightarrow \tfrac{2}{5}N_2 + HCO_3^- + (1-\gamma)H^+ + \gamma NH_4^+ + \tfrac{2}{5}H_2O \tag{7}$$

$$R_3 : NH_4^+ + 2O_2 \rightarrow NO_3^- + 2H^+ + H_2O \tag{8}$$

$$R_4 : \{NH_3\}_{OM} + H^+ \rightarrow NH_4^+ \tag{9}$$

In these reactions, $\{CH_2O\}\{NH_3\}_\gamma$ represents organic matter with γ the N:C ratio of organic matter. The rates of aerobic respiration and denitrification were modeled using the classical formulation for electron acceptors (Meysman *et al.,* 2003).

$$R_1 = \frac{C_{O_2}}{C_{O_2} + K_{O_2}^{sat}} R_{\min} \tag{10}$$

$$R_2 = \frac{K_{O_2}}{C_{O_2} + K_{O_2}^{sat}} \frac{C_{NO_3^-}}{C_{NO_3^-} + K_{NO_3^-}^{sat}} R_{\min} \tag{11}$$

In these expressions, $R_{\min}$ represents the mineralization rate of organic matter, which was assumed to be constant throughout the sediment domain (as a result of the initial homogenization of the sediment). The parameters $K_{O_2}^{sat}$ and $K_{NO_3^-}^{sat}$ are saturation constants, which were respectively set to 5 μmol L^{-1} and 30 μmol L^{-1} (following Cook *et al.,* 2006). The inhibition $K_{O_2}^{inh}$ represents the oxygen level above which denitrification is inhibited, and was set to 5 μmol L^{-1} (Cook *et al.,* 2006). Organic matter mineralization through other metabolic pathways such as Fe/Mn and sulphate reduction is not explicitly modeled, but accounted for through the ammonification reaction R_4, with associated rate $R_4 = \gamma R_{\min}$. Nitrification was modeled using the bimolecular kinetic rate

$$R_3 = k_N C_{O_2} C_{NH_4^+} \tag{12}$$

where k_N is the nitrification constant, which was initially set to 10 μmol L^{-1} yr^{-1} (but changed afterwards in the sensitivity analysis). Following Cook *et al.* (2006), our model assumes that the oxygen consumption from re-oxidation of reduced by-products other than ammonium (e.g., FeS_2, H_2S, Fe^{2+}) can be neglected. This assumption is partially justified by the relatively large values for the Respiratory Quotient (RQ—see Table 2 and data below). RQ values in the range 1.6–1.8 indicate that pyrite accumulation rather than pyrite re-oxidation occurs (the latter would bring RQ values closer to 1). Our model assumes that no ANaerobic AMMonium OXidation (ANAMMOX) and Dissimilatory Nitrate Reduc-

Table 1. Overview of parameter values used in the biogeochemical model simulations.

Symbol	Parameter	Mimic	Fresh worm	Acclimated worm	Units
R_c	Core radius	5.1	5.1	5.1	cm
H_s	Sediment height	18.5	19.6	20.1	cm
H_b	Height of burrow	12.0	19	19	cm
R_b	Radius of burrow	1.0	0.4	0.4	cm
Q	Pumping rate	1.7	1.4	0.8	ml min^{-1}
R_{min}	Mineralization rate	142	123	67	mmol m^{-2} d^{-1}
Concentration in the overlying water					
C_{O2}^{ow}	O_2	233.0	235.2	234.4	μmol L^{-1}
C_{HCO3-}^{ow}	HCO_3^-	2469	2504	2491	μmol L^{-1}
C_{NO3-}^{ow}	NO_3^-	15.7	16.2	17.6	μmol L^{-1}
C_{NH4+}^{ow}	NH_4^+	9.2	10.3	10.4	μmol L^{-1}
C_{N2}^{ow}	N_2	420	420	420	μmol L^{-1}
ϕ	Porosity		0.40		
ρ_s	Solid sediment density		2.5		g cm^{-3}
γ	C/N ratio in organic matter		13		
K_{O2}	Saturation constant O_2		5		μmol L^{-1}
K_{NO3-}	Saturation constant NO_3^-		30		μmol L^{-1}
k_N	Kinetic constant for nitrification		$10 \sim 1000$		μmol L^{-1} yr^{-1}

tion to Ammonia (DNRA) take place. In a similar study on the influence of physically induced flow on N-cycling in sandy sediments, Cook *et al.* (2006) found that rates of ANAMMOX were negligible. Furthermore, in a comparable bio-irrigation study of *Corophium volutator,* Pelegri and Blackburn (1994) found that DNRA accounted for less than 5% of nitrate reduction. However, this does not preclude the possibility that ANAMMOX and DNRA could be important in our sediment, because both ANAM-MOX (Engström *et al.,* 2005) and DNRA (Kelly-Gerreyn *et al.,* 2001) have been found to be important in some coastal sediments. In fact, the principal reason for not including ANAMMOX and DNRA in our model formulation is the lack of appropriate isotope measurements that constrain the rates of these processes. All model parameters in our model are essentially constrained by experimental observations (no free fitting parameters), and so for each treatment, a single set of parameters is derived (an overview of the model parameters is given in Table 1).

f. Statistical analysis

All fluxes and rates in cores were statistically tested for differences between controls and irrigated cores (acclimated/fresh/mimic) using one-way analysis of variance (ANOVA). Homogeneity of variances was checked using Levene's test and when found to be heterogeneous, the data were log-transformed. In cases of significance of the ANOVA test, multiple comparisons between the means were made using Tukey's test. Differences were accepted as significant at the level $p < 0.05$.

3. Results

a. Sediment characteristics

At the conclusion of the experiment, sediment cores were vertically split. The sediment coloration pattern differed markedly between the four treatments (Fig. 2). The control cores showed a homogenous greyish-black coloration throughout the cores, with only a narrow (~2 mm depth) yellow-brownish oxidized zone of about 2 mm at the surface (Fig. 2a). The cores containing *A. marina* had a similar oxidized surface layer of about 3 mm depth, but also showed a similar oxidized zone around intersected burrows. A clearly distinguishable but narrow yellow-brownish zone (1–2 mm) was found surrounding the burrow over its entire length (Fig. 2b). This oxidized zone did not substantially widen near and around the feeding pocket. Near the opening of the J-shaped burrow, black faecal mounds covered the otherwise yellow-brownish surface. The sediment coloration pattern in the mimics was markedly different with a very wide (~15 mm in diameter) egg-shaped oxidized zone surrounding the feeding pocket (Fig. 2c).

There was no significant difference in porosity (0.40 ± 0.1), solid sediment density (2.5 ± 0.3 g cm^{-3}), organic carbon content ($0.4 \pm 0.1\%$), and C:N ratio (13.1 ± 0.4) before and after the experiment. There was no significant difference in these sediment parameters between treatments, nor was there any significant vertical zonation in these properties in the cores after the experiment. Values for these sediment parameters are summarized in Table 1. In the cores containing lugworms, the deeper core section (4–20 cm) was carefully examined to determine the radius R_b and the depth H_b of the feeding pocket. These burrow parameters showed no differences between the "fresh worm" and the "acclimated worm" treatments ($R_b = 0.4$ cm and $H_b = 19$ cm). In all cases, the lugworms burrowed down all the way, creating their feeding pocket close to the bottom of the core. In one of the cores of the "acclimated worm" treatment, no signs of oxidized burrow linings were observed, and the lugworm was found partially decomposed (indicating that it probably died immediately after being added to the core). This was confirmed by the results of the corresponding incubation, which showed no sign of bio-irrigation activity. Therefore, this core is excluded from the results and discussion section.

b. Irrigation rates

Figure 3 displays how the uranine concentration evolved over time after spiking the overlying water. All treatments show a good reproducibility between replicates. The control cores (Fig. 3a) show a small and linear decrease in the tracer concentration (7% over 36 hr incubation period). This slow and steady decrease is characteristic of diffusion across the sediment-water interface, and the subsequent accumulation of uranine in the pore water and its adsorption onto the sediment matrix. Previous studies have shown that stirring of the overlying water during incubations of sandy sediments can induce radial pressure gradients, thus generating advective exchange across the sediment-water interface (Glud *et al.,* 1996). However, this phenomenon is not observed at the stirring rates used in the present incubations. The shallow and radially uniform oxygen penetration depth as well
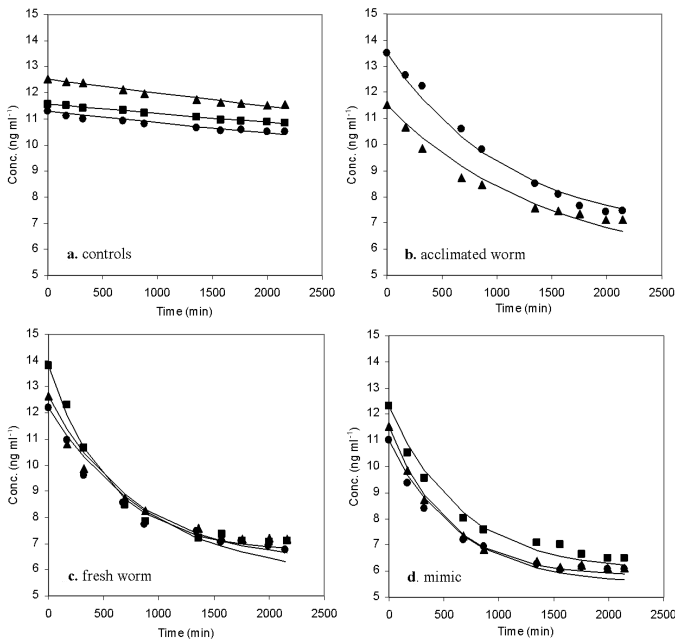
Figure 3. The evolution of the uranine concentration in the overlying water during incubations. Different markers denote different replicate incubations. The solid lines represent the best fit of the analytical bio-irrigation model (Eq. (4)) described in the text. These model fits provide an estimate for the bio-irrigation rate Q—see Table 2.

as the slow and linear tracer decrease (Fig. 3a), corroborate that molecular diffusion across the sediment-water interface is the dominant transport process of solutes in the control cores.

The uranine response in all the irrigated cores (acclimated: $p < 0.03$ / fresh: $p < 0.001$/ mimic: $p < 0.000001$) was significantly different from the controls (Fig. 3 b–c). The uranine concentration rapidly decreased and tended towards a constant concentration level at the end of the incubation period (indicating that pore water and overlying water are fully mixed). Advective irrigation thus results in a fast and efficient exchange of tracer between sediment and overlying water. Tracer-rich overlying water is injected at depth, and as a consequence, tracer-free pore water is pushed upward across the sediment-water interface. This advective exchange is far more rapid than the strictly diffusive mechanism in the control cores.

The initial concentration change (i.e., the time derivative of the tracer concentration at time zero) is largest in the mimics, followed by the fresh worm, and then the acclimated worm cores. Overall, the simple analytical model Eq. (4) provided an excellent fit to the data profiles (Fig. 3). As noted before, in these model fits, all parameters (C_{OW}^{o}, R_C, H_{OW}, H_S, ϕ, ρ_S, K_{ad}) are constrained *a priori* by measurements, except for the irrigation rate Q, whose value is calibrated to provide the best fit. The irrigation rate for the continuously

pumping mimics (1.7 ± 0.2 ml min^{-1}) was close to the directly measured pumping rate (2.1 ± 0.1 ml min^{-1}). At the same time, the irrigation rate of the mimics was slightly higher than that of the fresh worms (1.4 ± 0.4 ml min^{-1}), but markedly higher than in the acclimated worm treatment (0.8 ± 0.1 ml min^{-1}) (Table 2). Not surprisingly, the irrigation rate was very low in the control cores (0.1 ml min^{-1}). These estimates for Q in the acclimated, fresh and mimic cores are within the range of pumping rates reported for *A. marina* in previous laboratory incubation experiments (1.5 ml min^{-1} in Riisgård *et al.,* 1996; 0.9 ml min^{-1} in Timmermann *et al.,* 2006).

c. Benthic fluxes

Advective bio-irrigation clearly increases the total oxygen uptake (TOU) rates of the sediment (Fig. 4a). The TOU in fresh worm (63.1 ± 19.7 mmol m^{-2} d^{-1}: p<0.01), and mimic treatment (90.3 ± 2.4 mmol m^{-2} d^{-1}: p<0.001) is significantly higher than in the controls (24.8 ± 0.9 mmol m^{-2} d^{-1}). On other hand little difference is seen between the acclimated worm (37.1 ± 5.1 mmol m^{-2} d^{-1}:p<0.6) and control. (Table 2). Stated otherwise, the TOU is enhanced by 50%, 155%, and 265% in the acclimated worm, fresh worm and mimic treatments respectively, as compared to the controls. The TOU in the controls is only sustained by diffusive oxygen uptake (DOU) across the sediment-water interface (i.e., TOU = DOU). Consequently, if one considers the TOU in the controls as a proxy for the DOU in the other treatments, one can calculate the Faunal Mediated Oxygen Uptake (FMOU) as FMOU = TOU − DOU. This calculation shows that the FMOU accounts for 30~70% of the TOU in the irrigated cores (Table 2—Fig. 4a).

The N_2 production rates were also substantially different between treatments and followed the same pattern as the FMOU rates: bio-irrigation strongly stimulates the N_2 production (Fig. 4b). The N_2 production rates were respectively 2.6, 4.3 and 9.7 times higher in the acclimated worm (p<0.19), fresh worm (p<0.007) and mimic treatments (p<0.00001), when compared to the controls (Table 2—Fig. 4b). In a similar way as was done for the Fauna Mediated Oxygen Uptake (FMOU), we calculated the Fauna Mediated N_2 Production (FMN$_2$P) by subtracting the N_2 production rate in the controls from the N_2 fluxes that were measured in the irrigated cores. The FMN$_2$P respectively accounts for 62%, 77%, and 90% of the total N_2 production in the acclimated worm, fresh worm and mimic treatments.

Net DIN (NH_4^+, NO_3^-) fluxes varied considerably between treatments and showed no consistent trend with the bio-irrigation rate. Overall, bio-irrigation had a limited effect on the DIN exchange, except for the very large ammonium efflux observed in fresh worm cores (Table 2—Fig. 4c). This fresh worm treatment also showed a large TCO_2 release (Fig. 4d). The most likely explanation for these high fluxes of DIN and TCO_2 is a non-steady state effect. Recall that the lugworms were added only 48 hr prior to the start of the incubation in this fresh worm treatment. Most likely, on addition of the lugworms, some transient outflushing of diagenetic end products occurred, which had accumulated in deeper sediment layers. Nonetheless, the duration of this outflushing is somehow incompat-

Table 2. Benthic fluxes and bio-irrigation rates obtained from microcosm incubations. Negative values for NH_4^+ and NO_3^- indicate fluxes into the sediment. The FMOU and FMN_2P are also expressed as their relative contribution (%) to the TOU and TN_2P respectively. Values represent the mean of 3 replicates. Error bars denote Standard Error.

| Flux or rate	Symbol	Units	Control	Acclimated worm	Fresh worm	Mimic
Irrigation rate	Q	$cm^{-3}\ ml\ min^{-1}$	0.1 ± 0.0	0.8 ± 0.1	1.4 ± 0.4	1.7 ± 0.2
Total O_2 uptake rate	TOU	$mmol\ m^{-2}\ d^{-1}$	24.8 ± 0.9	37.1 ± 5.1	63.1 ± 19.7	90.3 ± 2.4
Fauna-mediated O_2 uptake rate	FMOU	$mmol\ m^{-2}\ d^{-1}$	0 (0%)	12.3 (33%)	38.3 (61%)	65.5 (73%)
FMOU/DOU ratio	—	—	0.0	0.5	1.5	2.6
O_2 input by pumping	$Q*[O_2]_{ow}$	$mmol\ m^{-2}\ d^{-1}$	3.12	34.8	58.6	68.8
Modified irrigation rate	$Q_{mod} = FMOU/[O_2]_{ow}$		0.0	0.3	0.9	1.6
TCO_2 flux		$mmol\ C\ m^{-2}\ d^{-1}$	47.1 ± 8.0	67.4 ± 40.9	606.1 ± 240	140.8 ± 19.5
Respiratory Quotient	TCO_2/TOU		1.9 ± 0.4	1.8 ± 0.9	9.5 ± 1.2	1.6 ± 0.2
NH_4^+ flux		$mmol\ N\ m^{-2}\ d^{-1}$	-0.4 ± 0.7	4.7 ± 7.9	52.3 ± 25.2	1.1 ± 3.2
NO_3^- flux		$mmol\ N\ m^{-2}\ d^{-1}$	-3.1 ± 1.8	-3.9 ± 4.6	0.8 ± 2.4	-3.2 ± 4.0
N_2 production	TN_2P	$mmol\ N\ m^{-2}\ d^{-1}$	1.8 ± 0.4	4.7 ± 3.4	7.7 ± 0.9	17.4 ± 1.0
Faunal Mediated N_2 production	FMN_2P	$mmol\ N\ m^{-2}\ d^{-1}$	0 (0%)	2.9 (62%)	5.9 (77%)	15.6 (90%)
FMN_2P/DN_2P ratio			0.4	1.6	3.3	8.7
DIN input by pumping	$Q_{mod}*[DIN]_{ow}$	$mmol\ N\ m^{-2}\ d^{-1}$	0.4	1.5	4.4	7.34
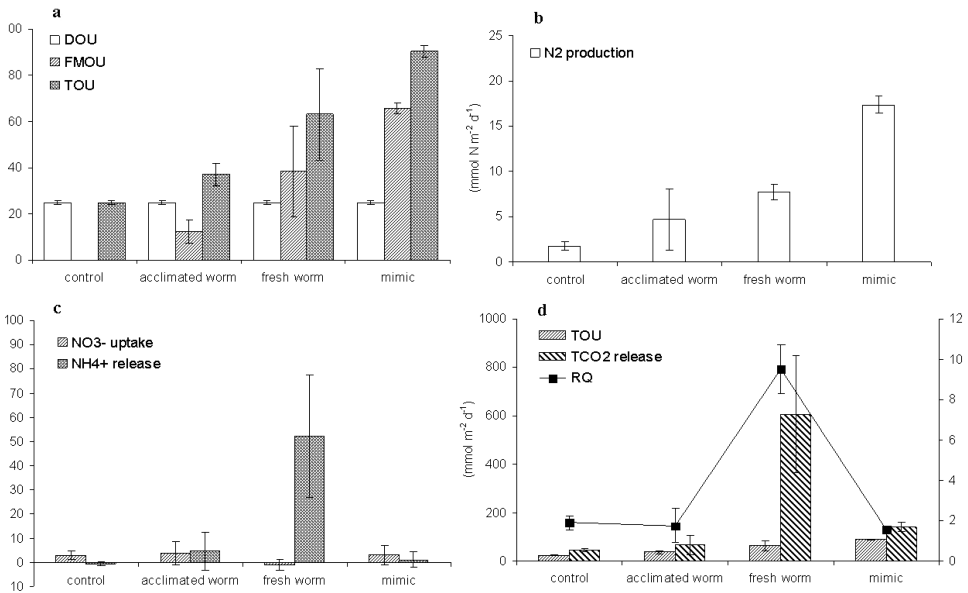
Figure 4. Benthic fluxes obtained from the incubations in the four different treatments. (a) Diffusive O_2 Uptake (DOU), Fauna-Mediated O_2 Uptake (FMOU), Total O_2 Uptake (TOU) (b) N_2 production (c) NH_4^+ release and NO_3^- uptake (d) Total CO_2 release (TCO_2) and Respiratory quotient (RQ). Values are presented as the mean of 3 replicates. Error bars denote Standard Error.

ible with the results of Figure 3c. This figure shows that for uranine, such transient effects were no longer present after 36 hr. Note however that uranine acts as a conservative tracer, and so its time evolution in the overlying water is only governed by transport. In contrast, the time response of DIN and TCO_2 is both governed by transport and reaction processes within the sediment: for a reactive solute, this can increase the time period needed to reach steady state. The TCO_2:TOU ratio or Respiration Quotient (RQ) was 1.6 in the mimic and to 1.8 in the acclimated worm, similar to the value of 1.9 in the controls. These RQ values are within the range of 1.0 to 4.0 in natural systems (Raine and Patching, 1980). The RQ value in the fresh worm treatment is extremely high (9.5), due to the extreme outflushing of TCO_2 mentioned above.

Both FMOU and FMN_2P strongly increased with increasing bio-irrigation rate Q (Fig. 5 a–b). This trend suggests that the more substrate (respectively O_2 or DIN) that is delivered to the sediment, the higher the accompanying rate of the metabolic transformation (respectively O_2 consumption and denitrification). To investigate this hypothesis in more detail, we calculated the actual oxygen/nitrogen input by pumping (Fig. 5 c–d). The O_2 input by pumping (mmol m^2 d^{-1}) is obtained by first multiplying the average O_2 concentration in the overlying water during the incubation (mmol ml^{-1}) with the bio-irrigation rate Q (ml d^{-1}) and subsequently dividing by the surface area of the core (m^2). The N input by pumping is calculated in the same way, but now the average

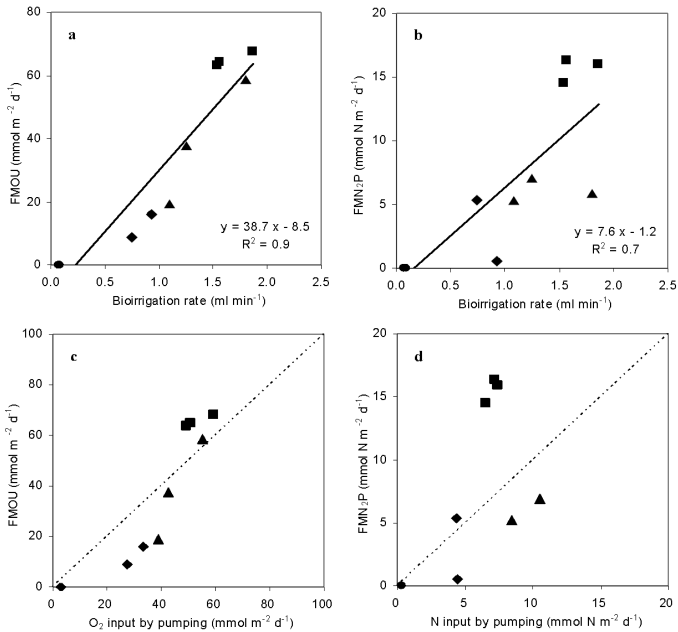Figure 5. (a–b) Fauna-Mediated O_2 Uptake (FMOU) and Fauna-Mediated N_2 Production (FMN_2P) as a function of the bio-irrigation rate Q. (c–d) FMOU and FMN_2P as a function of the oxygen and nitrogen input respectively (see text for the calculation of these latter quantities). Markers denote different treatments (● control, ◆ acclimated worm, ▲ fresh worm, ■ mimic). Trend lines in (a–b) are drawn using least-squares linear regression. The 1:1 lines in (c–d) are shown for comparison.

concentration of DIN ($NH_4^+ + NO_2^- + NO_3^-$) in the overlying water is used. Note that this calculation assumes that all ammonium and nitrite entering the sediment will eventually be used as substrate for N_2 production.

The 1:1 line (dotted line) in Figure 5c corresponds to a situation where the FMOU exactly matches the oxygen input by pumping. In the absence of benthic photosynthesis, the overlying water provides the only source of oxygen to the sediment. Accordingly, we can assume that all the oxygen contained within the incoming burrow water is completely consumed upon passage through the sediment (either by lugworm respiration or by microbial oxygen consumption in the sediment). Hence theoretically, all oxygen data should fall close to the 1:1 line. This is indeed the case for the all mimic cores and two of the three fresh worm cores. In contrast, the acclimated worm cores and a single fresh worm core show FMOU rates that are only half of the expected value based on oxygen input. One possible explanation for this discrepancy could be that the estimates for the bio-irrigation rate Q and FMOU are obtained from different incubations. Perhaps lugworms were pumping less strongly during the (closed) oxygen incubations, than during the (open) uranine incubations. Yet overall (and accounting for some analytical uncertainty), the correspondence between oxygen input and FMOU is rather good. Such correspondence is

not obtained when we compare the Faunal Mediated N_2 production (FMN$_2$P) and nitrogen input through pumping. Here, the data substantially deviate from the theoretical 1:1 line (Fig. 5d). This is not really surprising, as there are many more factors that can cause deviations from the 1:1 line in the case of N_2 when compared to O_2. Foremost, there are two sources of DIN to the sediment: either transport from the overlying water (the external DIN input) or internal generation through the organic matter mineralization (the internal DIN input). Hence, one will only approach the 1:1 line when denitrification is exclusively sustained by the external DIN input. Strikingly, the mimic cores show much larger FMN$_2$P values than expected based on DIN input. In contrast, the worm treatments (acclimated worms and fresh worms), which show a lower bio-irrigation rate, stimulate the FMN$_2$P far less than the mimic treatment. As discussed in more detail in the next section, this difference in FMN$_2$P between mimics and worm treatments is suitably explained by a strong difference in the rate and regulation of coupled nitrification-denitrification.

d. Biogeochemical model simulations and sensitivity analysis

Using the biogeochemical model outlined in Section 2e, we performed steady-state simulations to examine the C and N-cycling in the various treatments. For each simulation, the model output consists of velocity fields, concentration patterns, reaction rates in the sediment, and solute fluxes to the overlying water. A subset of these rates and fluxes were measured in the experimental incubations (oxygen consumption, denitrification, solute fluxes). Figure 6 shows the model output for two specific simulations that will be discussed in detail below: model scenario 1 (mimic) and model scenario 7 (acclimated worm) of Table 3. Two-dimensional concentration patterns for the solutes O_2, NO_3^-, NH_4^+, and the associated spatial distribution for oxygen consumption, denitrification, and nitrification are shown.

Each model simulation is based on a specific parameter set (an overview is given in Table 1). As noted above, the majority of these parameter values are based on direct measurements. These include sediment characteristics (porosity, solid sediment density, C/N ratio) and the parameters that define the geometry of the model domain (core radius R_c; sediment height H_s; height of burrow H_b; burrow radius R_b). The depth-integrated mineralization rate R_{min} was set to the average TCO$_2$ flux measured in each treatment (assuming no dissolution or precipitation of carbonates). To obtain the ammonium release rate N_{min} we divided the mineralization rate R_{min} by the C/N ratio. The concentrations of solutes in the overlying water were set to those measured at the start of the incubations. The only parameters that were based on literature data are the saturation and inhibition constants for oxygen and the constant for nitrate (Cook *et al.*, 2006).

A sensitivity analysis (as discussed in detail below) revealed that the simulation output was particularly sensitive to changes in the two remaining parameters: the nitrification constant k_N and the pumping rate Q. Unfortunately, these two parameters were also the parameters that were the least constrained by data. The value of k_N was initially set to the value of 10 μmol L^{-1} yr^{-1} as used in previous biogeochemical model applications (Wang and Van Cappellen, 1996; Cook *et al.*, 2006). There is however no a priori reason why the

a. Mechanical mimic

b. Acclimated worm

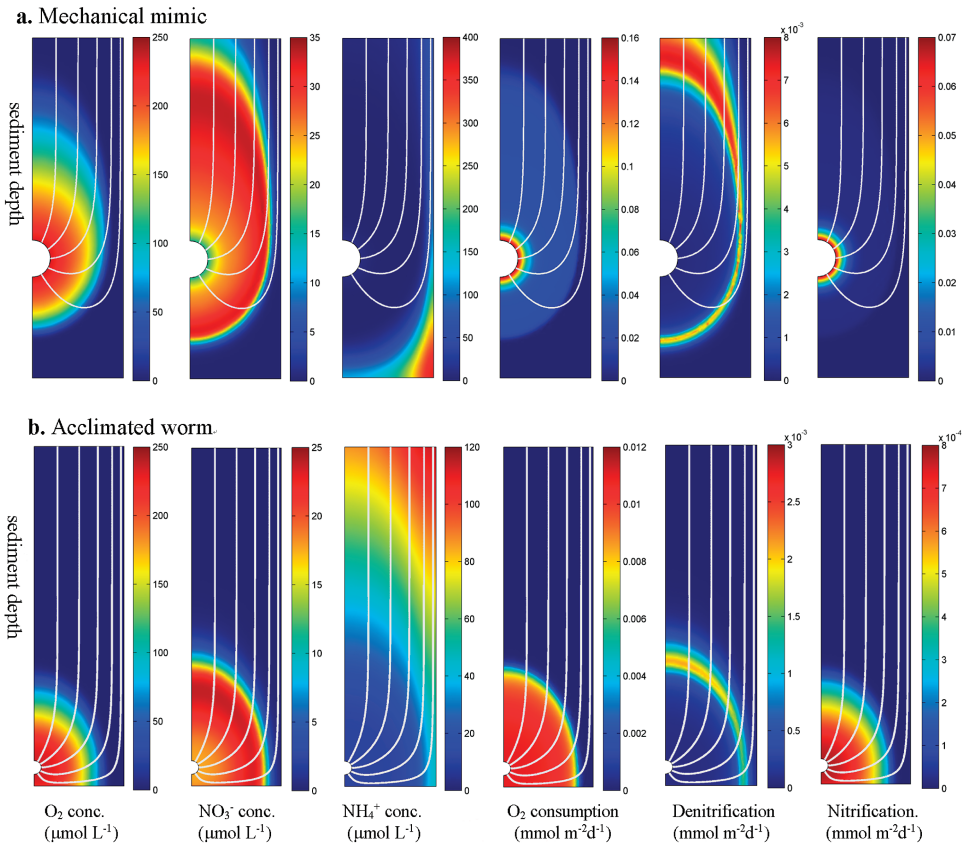| O₂ conc. (μmol L⁻¹) | NO₃⁻ conc. (μmol L⁻¹) | NH₄⁺ conc. (μmol L⁻¹) | O₂ consumption (mmol m⁻²d⁻¹) | Denitrification (mmol m⁻²d⁻¹) | Nitrification. (mmol m⁻²d⁻¹) |

Figure 6. Simulation output of the biogeochemical N-cycling model which generates velocity fields and concentration patterns in the sediment environment surrounding the lugworm's burrow. Core patterns indicate the spatial distribution of solute concentrations (O_2, NO_3^-, NH_4^+) and reaction rates (oxygen consumption, denitrification, and nitrification) for (a) mimic and (b) acclimated worm treatment. White lines represent the simulated flow line pattern.

intrinsic nitrifying activity of the microbial community, as exemplified by k_N, should be constant across model applications. The bimolecular rate law (10) is in fact a strong simplification of a complex microbial process, and so, there is no guarantee that this particular mathematical rate law forms an appropriate description for nitrifying activity. Secondly, a different type of uncertainty affected the pumping rate Q. As noted above, the FMOU data in these treatments were lower than expected based on the oxygen input (see Fig. 5c). This indicates that the Q values derived from the uranine method presumably overestimated the true pumping rate in the fresh worm and acclimated worm treatments. To match the FMOU data, one needs a lower oxygen input, and this requires a decrease of the pumping rate Q.

Because of this uncertainty associated with k_N and Q, we did not treat these two parameters like the other parameters, which were assigned fixed "known" values. Instead

Table 3. The output of model simulation. Oxygen and nitrogen were supplied to sediments from the overlying water in the model by pumping, two variable parameters, the nitrification rate constant (k_N) and pumping rate (Q).

	Mimic			Fresh worm		Acclimated worm	
Model Scenarios	1	2	3	4	5	6	7
k_N (μM^{-1} yr^{-1})	1000	100	10	100	10	100	10
Pumping rate (ml min^{-1})	1.7	1.7	1.7	0.9	0.9	0.3	0.3
Reaction rates (mmol m^{-2} d^{-1})							
O$_2$ consumption	68.6	68.3	68.2	22.1	22.1	11.7	11.7
Aerobic mineralization							
Denitrification	9.8	8.2	4.9	3.6	2.5	1.9	1.3
Nitrification	6.8	5.0	1.4	2.0	0.9	1.1	0.5
Net flux (mmol m^{-2} d^{-1})							
NH$_4^+$ Out	4.0	5.9	9.5	3.1	4.2	4.0	4.6
NO$_3^-$ In	3.0	3.2	3.5	1.7	1.7	0.9	0.9

we explored a reasonable parameter range, where k_N was given three values (10, 100, 1000 μmol L^{-1}yr^{-1}) and Q was also given three values (100%, 70% and 30% of the bio-irrigation rate Q measured in the uranine incubations). Performing 9 simulations for each of the three treatments (mimic, fresh worm, and acclimated worm) thus resulted in a total of 27 simulations. Table 3 depicts the output for a representative set of 7 simulations.

e. Data-model comparison and N mass balances

In order to compare the experimental data with the output of the model simulations, we constructed two separate nitrogen mass balances for each treatment: one "experimental N balance" based on the experimental flux data, and one "model N balance" based on a corresponding model simulation (Fig. 7). To construct the experimental N balance, we assumed steady state conditions. To arrive at a full scheme, missing (i.e. non-measured) fluxes were inferred by mass balance. Subsequently, out of the 9 available model simulations for each treatment, the model N balance was selected that gave the closest correspondence to the experimental N balance. For both the acclimated worm and mimic treatment, we were able to construct a closed experimental N balance, and we also found a suitable model N balance that closely reproduced the measured experimental fluxes (Fig. 7). This was not possible for the fresh worm treatment, because of the non-steady state situation. No sensible experimental N balance could be constructed due to the extreme high outflux of ammonia, and likewise, no matching steady state simulation could be associated. Accordingly, the simulation results of the fresh worm treatment are not considered any further. For the mimic, the best fit was obtained in model scenario 1 (Table 4), where the irrigation rate was set as measured from the uranine incubations, but the nitrification constant k_N was increased to 1000 μmol L^{-1} yr^{-1}. Note that this best model scenario still
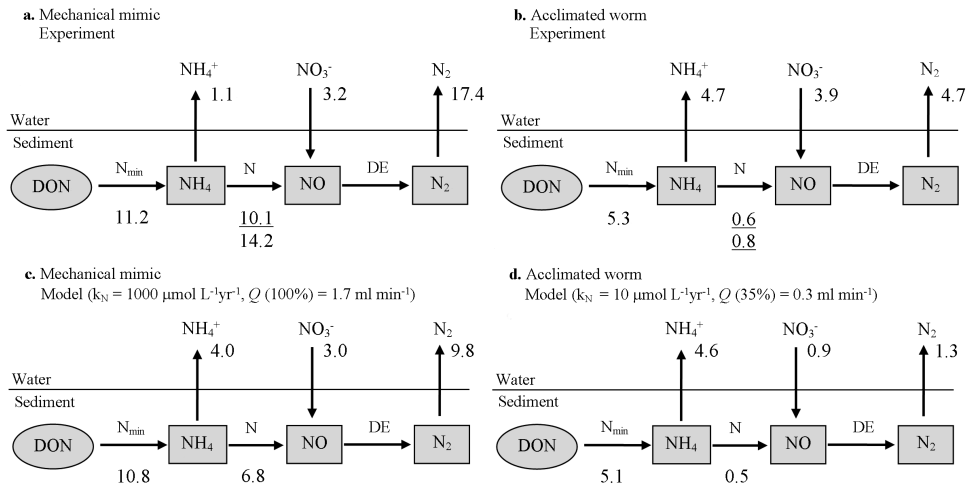
Figure 7.   Nitrogen cycling schemes showing benthic fluxes of ammonium, nitrate and N_2. Denitrification rates (DE); Nitrification (NI), Nitrogen release-mineralization rate (N_{min}). Underlined values are inferred from mass balance conservation (upstream or downstream).

predicts a higher outflushing of NH_4^+, a lower nitrification rate and a lower denitrification rate. Increasing the nitrification constant k_N to values beyond 1000 μmol L^{-1} yr^{-1} could not alleviate this discrepancy. In the acclimated worm scenario, the best fit was obtained in model scenario 7 (Table 4), where k_N was kept at the baseline value of 10 μmol L^{-1} yr^{-1}, but the irrigation rate Q was decreased from 0.8 to 0.3 ml min^{-1}. Here, the model predicts a lower influx of NO_3^-, and also a lower overall denitrification rate.

f. Sensitivity analysis

Changing the k_N and Q for the various treatments (mimic, acclimated worm, and fresh worm) had a marked effect on oxygen consumption and N–cycling (results are summarized in Table 4). When properly translated, this parameter sensitivity analysis enables insight in the (complex) interplay between advective irrigation, microbial ecology and sediment biogeochemistry. From a purely geochemical perspective, the irrigation rate Q represents the intensity of pore water transport, while in ecological terms, Q serves as a proxy for the macrofaunal activity. Similarly, in geochemical terms, the kinetic constant k_N quantifies the reactivity of the sediment, while in terms of microbial ecology, it serves as a proxy for the activity of nitrifying micro-organisms per unit volume of sediment.

Table 4. Summary of sensitivity test of reactive transport model.

	O_2 cons.	Nitri	Denitri	NH_4^+	NO_3^-
Nitrification constant k_N	↑	0	↑↑	↑	↓↓	0
Pumping rate (Q)	↑	↑	↑	↑	↓	↑

An increase in the nitrification constant k_N at a constant bio-irrigation rate Q (row 1 in Table 4) does not increase the oxygen consumption in the sediment. This result may seem counterintuitive at first sight, since the oxygen concentration features in the bimolecular rate law (Eq. 10). However, on closer inspection, the total oxygen uptake within the sediment is limited by the supply of oxygen to the sediment. The total oxygen uptake to the sediment (TOU) is composed of the diffusive input across the sediment water interface (DOU) and the advective oxygen input by pumping (FMOU). These two components will react differently to an increase in k_N. The DOU will be sensitive, since an increase in k_N implies a higher demand for oxygen within the sediment, resulting in a decreased oxygen penetration depth, and hence an increased diffusive flux. In contrast, the oxygen input by pumping (FMOU) is only dependent on the concentration of oxygen in the overlying water and the pumping rate Q, and thus remains insensitive to changes in the reactivity of oxygen (exemplified by k_N). In our simulations of the irrigated cores, the diffusive input (DOU) forms only a smaller contribution and the TOU is dominated by the oxygen input by pumping (FMOU). This explains why the TOU is relatively insensitive to the intrinsic reactivity of oxygen within the sediment (especially at the high irrigation rates of the fresh worm and mimic treatments).

The sensitivity analysis also shows that an increase in the nitrification constant k_N strongly stimulates the N cycling. The depth-integrated nitrification rate strongly increases, with a concurrent stimulation of the denitrification rate, and a concomitant reduction in the ammonium outflux from the sediment (first row of Table 4). Accordingly, when the nitrification constant k_N increases, more ammonium (either internally released from mineralization or supplied from the overlying water column through pumping) is captured and converted to nitrate, which increases the availability of nitrate in the sediment, thus stimulating denitrification. At the same time, ammonium concentrations are lowered in the pore water, and hence, less ammonium is carried along with the upward pore flow that returns to the water column.

The effects of a varying bio-irrigation rate Q at a constant nitrification k_N (second row of Table 4) can be explained along very similar lines. An increase in the pumping rate Q will increase the TOU because it increases the advective oxygen input by pumping (FMOU). This will increase the oxygenated zone within the sediment where ammonium comes into contact with oxygen (around the burrow and particularly near the feeding pocket—see Fig. 2c). This results in increased nitrification, which then stimulates denitrification through coupled nitrification-denitrification, and reduces the outflow of ammonium from the sediment. Note that in this scenario, nitrification is stimulated by increasing the spatial niche for nitrifying activity (the oxygenated zone) and not by increasing the inherent microbial reactivity (because the parameter k_N is kept constant). Consequently, our model sensitivity analysis shows that there are two distinct ways to stimulate nitrification: (1) the stimulation of the intrinsic microbial activity of the nitrifiers (increasing k_N at constant Q) and (2) increasing the bio-irrigation rate and hence the O_2 supply to the sediment (increasing Q at constant k_N) which increases the zone of nitrification.

4. Discussion

a. Methodological aspects: Laboratory incubations with large macrofauna

The common approach to study the role of infauna on sediment biogeochemistry has been through manipulated laboratory microcosms. In one type of experiments, the sediment is sieved to remove the ambient macrofauna, and selected species are introduced at known densities (e.g., Banta *et al.,* 1999; Mermillod-Blondin *et al.,* 2004; Papaspyrou *et al.,* 2007; the approach used in this study). A variant approach brings back intact cores to the laboratory, kills off existing benthic macrofauna by asphyxiation, but retains sediment integrity and natural chemical gradients, and then adds selected species at known densities to these intact cores (e.g., Hansen and Kristensen, 1997; Tang and Kristensen, 2007). Whatever the method used, the addition of strongly bio-irrigating organisms to a sediment core will typically induce a strong non-steady state response. In our study here, we examined both the flushing response immediately after the introduction of the bio-irrigator (fresh worm treatment: lugworm acclimation period of 2 days) as well the longer-time response of continued bio-irrigation (acclimated worm treatment: lugworm acclimation period of 22 days). The fluxes in the fresh worm treatment are large and have a clear non-steady state signature, and consequently, no matching steady-state N balance could be constructed. In contrast, the fluxes in the acclimated worm treatment are smaller, and could be fitted into a steady-state scheme of N cycling (Fig. 7b). Our results thus confirm the characteristic pattern observed in microcosm studies of bio-irrigating macrofauna (e.g., Banta *et al.,* 1999; Papaspyrou *et al.,* 2007). Large fluxes are observed immediately after the introduction of the organisms, and these fluxes subsequently attenuate to lower, constant baseline value over time (e.g. 16 days for O_2 consumption and TCO_2 fluxes in *A. marina* incubations of Papaspyrou *et al.,* 2007). This transient high-flux regime is caused by diagenetic products that have accumulated in deeper layers, which are flushed out of the sediment upon the introduction of the bio-irrigator.

In theory, non-steady state effects can be avoided by increasing the acclimation period of the organisms prior to incubation. However, our results show that increasing this acclimation period also has an important downside. Comparing the fresh worm and acclimated worm treatments, the bio-irrigation rate Q strongly decreases with a concomitant effects on fluxes and rates (moreover, one of the three lugworms in the acclimated worm treatment even died). Prolonged incubation implies that the organism has to survive in a rather artificial sediment environment, which lacks natural ecological interactions and ambient hydrodynamic conditions (such as erosion/resuspension cycles, and tidal currents). Most importantly, laboratory conditions in continued darkness are unfavourable to the macrofauna because they lack the natural food supply (settling of fresh organic matter, and primary production by microphytobenthos). Overall, it is however inherently difficult to assess how well the irrigation activity observed in lab incubations represents the "average" field situation. Bio-irrigation and burrowing activity shows a clear seasonal signal (e.g. Maire *et al.,* 2007), as well as patterns in activity over time scales of days, hours and even minutes (e.g. Wenzhöfer and Glud, 2004; Wethey *et al.,* 2008).

In conclusion, there seems to be an inherent dilemma underlying microcosm bio-irrigation experiments. On the one hand, one requires a sufficiently long acclimation period to avoid the transient outflushing of the sediment immediately after the introduction of the animal. Yet on the other hand, our measurements show that the length of the acclimation period decreases the irrigation intensity of the organisms. This implies that incubations with long acclimation periods may underestimate the ambient geochemical effects of bio-irrigation. Because of this, great care should be taken when extrapolating the results of laboratory microcosm studies on bio-irrigation to geochemical cycling in the field.

b. Mechanical mimics of advective bio-irrigation

Until now, burrow mimics have only been used occasionally in sediment studies, and in those studies, they have been typically implemented to simulate the effect of radial diffusion to and from the burrow (Forster and Graf, 1992; Marinelli *et al.,* 1994). Here we have compared a mechanical mimic that simulates advective pore flow to the actual bio-irrigational effects of real lugworms. Overall, mimics have several advantages over live organisms, especially when the aim is to reduce variability in order to target specific geochemical processes and mechanisms. Firstly, the burrow geometries of lugworms (but also other dominant bio-irrigators in coastal sediments like *Thaliannassid* shrimp) are typically large compared to the size of currently employed incubation cores (which are typically $\sim$10 cm in diameter and $\sim$20 cm in length). In our incubations, we observed that lugworms were attracted to walls and the bottom of the core (Fig 2a). Mimics do not show such container effects: the feeding pocket can be placed exactly in the centre of the sediment core at the preferred height. Secondly, in contrast to live organisms, mimics are not negatively affected by prolonged incubation (see discussion above). Thirdly, mimics substantially reduce the variability in rates and fluxes when compared to the use of actual bio-irrigating organisms in incubation experiments. Table 2 and Figures 4–5 clearly illustrate this: the standard deviations in the mimic treatment are considerably smaller than in the fresh and acclimated worm treatments. Fourthly, mimics allow a much tighter control on the bio-irrigation rate Q, which can be fixed at any desired value.

Given these advantages, a crucial question is how accurately does the mechanical mimic reproduce the bio-irrigation effects of real lugworms? Following distinctions hold: (1) the mimic strictly simulates the bio-irrigation effects of the lugworm, but does not account for the effects of particle mixing. (2) The mimic continuously pumps at a constant rate, while actual lugworm pumping is intermittent and temporal variable (Kristensen, 2001). (3) In our present set-up, the "burrow" water in the mimic is identical to the overlying water: there is no diffusion of O_2 or other solutes across the burrow wall, and the mimic does not account for any respiration or excretion activity. This is an important difference when comparing the biogeochemical effects between mimics and real lugworm. Based on a detailed O_2 budget for a lugworm burrow system, Timmermann *et al.* (2006) estimated that 49% of the oxygen pumped into the burrow was consumed by the respiration of the lugworm itself, 23% of the oxygen was lost by diffusion across the burrow wall, and only

28% of the oxygen input was delivered to the sediment by the advective flow across the feeding pocket. Based on model simulations, these authors also hypothesized that under normal sediment conditions, oxygen would be rapidly consumed beyond the feeding pocket and not be advected back to the overlying water. Our experimental results corroborate these arguments. Although the pumping rate Q and the advective oxygen input are comparable in the mimic and fresh worm treatment, the fresh worm core only shows a small oxic "halo" around the feeding pocket, while the mimic core shows a large oxidized zone (which however does not reach the sediment surface). In addition, the fresh worm core shows a clear oxidized lining around the burrow, which is absent in the mimic treatment. These results indicate that the respiration of the lugworm together with radial diffusion must substantially reduce the oxygen level of the burrow water before it is pumped into the sediment across the surface of the feeding pocket. Rather simple modifications of the present mimic set-up could provide a more realistic simulation of lugworm bio-irrigation (permeable tubing that allow radial diffusion across the burrow wall, an O_2 "trap" in series with the pump that reduces the O_2 concentration in the burrow water, and hence, mimics the respiration of the lugworm by removing a fraction of the O_2).

Despite these differences between actual lugworm bio-irrigation, the mimic does an excellent job at mimicking the biogeochemical effects of advective bio-irrigation. This is immediately apparent from the similarity of the N cycling schemes displayed in Figure 7. A detailed discussion of the similarity in the rates between the mimic and lugworm treatments is given below. Accordingly, the mimic should be used for what it is: it does not emulate all aspects of lugworm bio-irrigation, but suitably targets the *advective aspect* of lugworm bio-irrigation. Therefore, we believe that mechanical mimics are a new and promising tool in bio-irrigation research.

c. Model-data comparison

Biogeochemical simulations allow a test of the consistency of the independently measured fluxes and rates. Both traditional mass balancing as well the model simulations revealed the high non-steady state nature of the fresh worm treatment. However, in the acclimated worm and mimic treatment, steady–state conditions were established, and a suitable closed N cycling scheme could be constructed (Fig. 7). The model simulations of the acclimated worm and mimic treatments provide a very similar pattern of rates and fluxes as in the experimental N cycling scheme (compare Fig. 7 a–c and b–d). The model estimates for the FMOU (mimic 68.6 mmol m^{-2} d^{-1}; acclimated worm 11.7 mmol m^{-2} d^{-1}) closely match the experimental values (mimic 65.5 mmol m^{-2} d^{-1}; acclimated worm, 12.3 mmol m^{-2} d^{-1}). A similar picture holds for the nitrogen fluxes, although some discrepancies exist between model and data. Because the flux data of ammonia and nitrate are poorly constrained (see large standard deviations in Table 2), the most significant difference is the systematic underestimation of the denitrification rate in the model. Despite a very high k_N value adopted in the model, the modeled N_2 production (mimic 9.8 mmol m^{-2} d^{-1}; acclimated worm 1.3 mmol m^{-2} d^{-1}) is consistently lower than the measured

Table 5. Summary of O_2 consumption (mmol m^{-2} d^{-1}) in lugworm microcosm incubations. Microcosm results are recalculated to a natural density of 40 ind. m^{-2} for adult lugworms and 120 ind. m^{-2} for juvenile lugworms.

	Microcosm duration (d^{-1})	DOU	TOU	FMOU	Microcosm density (ind. m^{-2})	Microcosm O_2 increase	Natural density (ind. m^{-2})	Natural O_2 increase
Fresh worm	2	24.8	63.1	38.3	122	154%	40	51%
Acclimated worm	22	24.8	37.1	12.3	122	50%	40	16%
Papaspyrou et al. (2007)	16	18	38.9	20.9	200	116%	120	70%
Banta et al. (1999)	20	27.9	103.4	75.5	600	260%	120	54%

FMN$_2$P (mimic 15.6 mmol m^{-2} d^{-1}; acclimated worm 2.9 mmol m^{-2} d^{-1}). This discrepancy clearly warrants further investigation. One option would be to conduct incubations with mimics at different pumping rates (as the model most closely describes the mimic set-up). Nonetheless qualitatively, our model simulations are accurate: they predict a much higher denitrification rate when the bio-irrigation rate is large. Overall, the biogeochemical model seems to capture essential features of nitrogen cycling within the sediment. This is remarkable given the strong simplifications in terms of model geometry and limited biogeochemical complexity that is incorporated in the model.

d. Influence of bio-irrigation on O_2 consumption and carbon cycling

The total oxygen uptake (TOU) of the sediment is strongly stimulated in the laboratory microcosms through advective irrigation, both by lugworms and mechanical mimics. The mimics caused the greatest enhancement of the TOU, resulting in an increase by 260% as compared to the defaunated controls (calculated as 100 × FMOU/DOU ratio). The presence of lugworms stimulated the TOU with 154% after 2 days of acclimation (fresh worm), which decreased to 50% after 22 days of acclimation (acclimated worm). These values are comparable to previous laboratory microcosm experiments with lugworms (Table 5), which reported a TOU increase of 116% after 16 days of acclimation (Papaspyrou *et al.,* 2007) and 260% after 20 days of acclimation (Banta *et al.,* 1999). However, these microcosm values pertain to different lugworm densities, which are also higher than the natural abundance (Riisgaard and Banta, 1998). Rescaling to a typical density of 40 ind. m^{-2} for adults or 120 ind. m^{-2} for juveniles, one finds that the TOU of the sediment is enhanced by 16–70% due to the presence of lugworms (Table 5). A similar stimulation of the TOU has been found for other dominant bio-irrigators of sandy coastal sediments. The activity of the burrowing shrimp *Callianassa subterranea* enhanced the TOU by 42% at natural densities in laboratory microcosm experiments with sandy North Sea sediments (Forster and Graf, 1995). Similarly, the mud shrimp *Corophium volutator* increased the TOU by 11–21% at densities 3000–6000 ind. m^{-2} (Pelegri and Blackburn, 1994). Higher values have been reported for the polychaete *Nereis diversicolor* (89%;

Banta *et al.,* 1999), the decapod shrimp *Trypaea australiensis* (81%; Webb and Eyre, 2004) and the brittle star *Amphiura filiformis* (147%; Vopel *et al.,* 2003). Similar to the TOU, bio-irrigation also stimulates the TCO_2 flux, and hence, organic matter mineralization. The increase of the TCO_2 flux in the acclimated worm (43%) and the mimic treatment (199%) are comparable with previous studies on lugworm bio-irrigation: 72 to 78% (Banta *et al.,* 1999) and 68% (Papaspyrou *et al.,* 2007).

Given this substantial stimulation of the TOU by advective bio-irrigation, one can investigate the mechanisms that are controlling the actual oxygen uptake. Theoretically, there are two possible end-member scenarios. In the case of *transport control,* the O_2 uptake is determined by the transfer rate of O_2 from the overlying water column, and the consumption of O_2 within the sediment adjusts itself to the available supply. In the case of *reaction control,* the O_2 uptake is determined by the reactivity of the sediment, and the O_2 supply adjusts itself to the O_2 demand by the reactive processes in the sediment. In sandy sediments, there is a fundamental difference between DOU and FMOU. The DOU resides under a tight reaction control: the higher the reactivity of the sediment, the shallower the oxygen penetration depth, the steeper the O_2 gradient at the sediment-water interface, and the higher the diffusive flux of O_2 into the sediment. In contrast, our analysis shows that the FMOU in the laboratory microcosms is governed by transport control. Because we separately determined the value of the bio-irrigation rate Q (via uranine incubation), we were able to calculate the oxygen input by pumping independently from the FMOU. Figure 5c shows that the FMOU roughly scales in a 1:1 fashion with the oxygen input by pumping. As a result, the TOU of a bio-irrigated sandy sediment can be decomposed as

$$TOU = DOU + FMOU = DOU + (Q/A)*[O_2]$$

where Q is the irrigation rate, $[O_2]$ is the oxygen concentration in the overlying water, and A is the surface area of the core. This demonstrates that the TOU is partly reaction controlled (the DOU part) and partly transport controlled (the FMOU part). The transport control of the FMOU part implies that the more oxygen is supplied to the sediment, the more oxygen is consumed. Similarly, when examining the influence of physically driven pore flow on sediment biogeochemistry, Cook *et al.* (2006) observed that a higher flushing rate (Q/A) corresponded to a higher O_2 consumption within the sediment. Since the FMOU comprises a dominant part of the TOU in the irrigated cores, advective irrigation thus exerts a strong control on O_2 consumption in sediments.

A subsequent question then is what mechanisms are responsible for the FMOU, i.e. where and how is the O_2 consumed: in the burrow or in the surrounding sediment? As noted above, part of the oxygen will be consumed by the respiration of the lugworm, and part of the oxygen will be consumed by microbial respiration along the tube walls and inside the sediment. Based on published values for the basal O_2 consumption of lugworms (1.13 μmol g^{-1} hr^{-1} at 22°C in Zebe and Schiedek, 1996; 1.15 μmol g^{-1} hr^{-1} at 15°C in Riisgård and Banta, 1998), we calculated the O_2 consumption due to respiration as 25–30 mmol m^{-2} d^{-1}. These are very high rates compared to the actually measured

FMOU values in the worm treatments (even exceeding the FMOU value in the acclimated worm treatment—Table 5). This discrepancy may originate in a number of ways. As discussed above, the conditions for the lugworm in the acclimated worm treatment were not optimal, with lower activity and lower respiration. Secondly, the allometric relations that we used are derived under idealized laboratory conditions (fully oxygenated chambers that contain no sediment), and this may overestimate the actual respiration as compared to *in situ* sediment conditions. Overall, our calculation does confirm that a substantial amount of the oxygen input by pumping must be consumed by lugworm respiration (49% was attributed to respiration by Timmermann *et al.*, 2006). This is further supported by the different extent of the oxidized zone between the mimic and lugworm treatments (compare Fig. 2 b and c).

The oxygen that is not consumed by lugworm respiration enters the sediment either by diffusion through the burrow wall or by advection through the surface of the feeding pocket. This oxygen can be consumed in two ways: (1) by stimulating the aerobic mineralization of organic matter or (2) by oxidizing a reservoir of reduced products (e.g. NH_4^+, pyrite) that has accumulated in anoxic sediment layers. Our experimental flux data show that the first scenario is more likely. Alongside the FMOU, the TCO_2 flux also increases, while the respiration quotient remains constant (Table 2: compare control, acclimated worm, and mimic). This indicates that the mineralization rate R_{min} increases with the bio-irrigation Q, and hence, with the increased O_2 input into the sediment. This suggests that advective bio-irrigation strongly stimulates the decomposition of organic matter through increased oxygenation of the sediment.

e. Effects of advective bio-irrigation on benthic N-cycling

The N_2 production rate showed a similar pattern as the TOU: the N_2 production rate was much greater in the irrigated cores than in the defaunated controls, and increased with the bio-irrigation rate Q. Our data thus confirm that lugworm bio-irrigation has a large effect on the N cycling in the sediment. To quantify this effect, we decomposed the total N_2 production (TN_2P) into a Diffusive N_2 Production (DN_2P—the N_2 production in the defaunated controls) and a Faunal Mediated N_2 Production (FMN_2P). This decomposition is analogous to that of the total oxygen uptake (TOU = DOU + FMOU). In all the irrigated cores, the FMN_2P constitutes the dominant component: the $FMN_2P:DN_2P$ ratio was 8.7 in the mimic, 3.3 in the fresh worm, and 1.7 in the acclimated worm treatment (Table 2). Such large enhancements of the N_2 production due to bio-irrigating macrofauna agree with previous observations: an *in situ* study of sediments inhabited by the shrimp *T. australiensis* showed that N_2 production was enhanced by a factor of 3.1 (Webb and Eyre, 2004), and a microcosm study of the benthic amphipod *C. volutator* showed an enhancement by a factor of 1.0 (Pelegrí and Blackburn, 1994).

Adopting a black-box perspective of sedimentary N cycling, there are two possible ways to increase the N_2 production (Nielsen, 1992; Henriksen and Kemp, 1998): (1) increasing the external supply of nitrate (or more generally of DIN) from the overlying water (2) enhancing the internal production of nitrate, and hence, stimulating the coupled nitrification-

Table 6. Summary of N_2 production in lugworm microcosm incubations based on the N cycling schemes in Figure 7. The total N_2 production is partitioned into a fraction based on NO_3^- derived from the water column and a fraction based on NO_3^- generated within the sediment.

	N_2 production	External nitrate input		Internal nitrification	
Experiment Mimic	17.4	3.2	18%	14.2	82%
Model Mimic	9.8	3.0	31%	6.8	69%
Experiment Acclimated worm	4.7	3.9	83%	0.8	17%
Model Acclimated worm	1.4	0.9	64%	0.4	29%

denitrification pathway. In previous studies on N cycling in faunated sediments, it was found that the contribution of nitrate from the overlying water accounts for more than 60–80% of total N_2 production (Jensen *et al.,* 1996; Karlson *et al.,* 2005). The N cycling schemes in Fig. 7 show a similar pattern for moderate irrigation rates, but suggest that the contribution of internal nitrification becomes more important when the irrigation rate increases. At the modest irrigation rate of the acclimated worm treatment ($Q \sim$ 0.3 ml min^{-1}), around three quarter of the N_2 production (63–84%; Table 6) is supported by external nitrate. However, when the irrigation rate increases in the mimic treatment ($Q \sim$ 1.7 ml min^{-1}), the situation changes and most of the N_2 production is supported by coupled nitrification-denitrification (only 17–29% supported by external nitrate; Table 6).

This high rate of coupled nitrification-denitrification at increased irrigation rates has also recently been observed in column experiments (Rao *et al.,* 2007, 2008), but nonetheless, it remains a rather puzzling observation. Advective irrigation is foremost a transport process, and hence, one would intuitively expect that at higher irrigation rates, N_2 production would be mostly stimulated via the external nitrate supply from the water column (Aller, 1988). However, this is not what happens in the mimic treatment. Nitrate values in the overlying water of our microcosms were relatively low ($\sim$10 µmol L^{-1}). Therefore, an increase in the irrigation rate Q only slightly increases the DIN input to the sediment. Figure 5d shows that the FMN_2P within the mimic treatment far exceeds the DIN input through pumping. Accordingly, bio-irrigation seems to enhance N_2 production mainly through stimulation of coupled nitrification-denitrification.

So what explains this increase in coupled nitrification-denitrification at higher irrigation rates? Our biogeochemical simulations show that there are three ways via which advective irrigation can stimulate coupled nitrification-denitrification (see also the sensitivity analysis section): (1) Increasing the endogenous release of ammonium by stimulating the mineralization rate of organic matter (increasing the parameter R_{min}); (2) Increasing the intrinsic activity of the microbial nitrifier population (increasing the parameter k_N); (3) Increasing the oxic volume (see Fig. 2c), and hence, enlarging the zone of nitrification within the sediment (i.e. increasing O_2 supply to the sediment through an increase in the parameter Q). When comparing the two N-cycling schemes in Figure 7, we find that advective irrigation stimulates nitrification-denitrification in all three ways. When compar-

ing the best model fits of the acclimated worm and mimic treatment, the oxygenation increased (because Q increases from 0.3 to 1.7 ml min^{-1}). However, Q was not the only parameter that needed modification. We also had to adapt the mineralization rate R_{min} from 67 to 142 mmol m^{-2} d^{-1}, which indicates that irrigation strongly stimulates organic matter mineralization through increased oxygenation. At the same time, we had to increase the k_N value from 10 to 1000 μM yr^{-1}, which indicates that irrigation stimulates nitrifier activity. In other words, our results suggest that in terms of biogeochemical consequences, a change in the advective irrigation rate of natural sediments entails a more complex response than that modeled by a simple adaption of the irrigation rate Q. Future experiments, using down-core profiling with flux measurements and stable isotopes, in combination with mimic incubations and biogeochemical modelling (as explored here), should provide a more detailed insight into this. Such investigations should also explore more detailed model representations of sedimentary N cycling, which investigate the importance of ANAMMOX and DNRA.

REFERENCES

Aller, R. C. 1988. Benthic fauna and biogeochemical processes in marine sediments: the role of burrow structures, *in* Nitrogen Cycling in Coastal Marine environments, T. H. Blackburn and J. Sørensen, eds., J. Wiley & Sons, New York.

—— 2001. Transport and reactions in the bioirrigated zone, *in* The Benthic Boundary Layer, B. P. Boudreau and B. B. Jorgensen, eds., Oxford University Press, 269 pp.

Aller, R. C. and J. Y. Aller. 1998. The effect of biogenic irrigation intensity and solute exchange on diagenetic reaction rates in marine sediments. J. Mar. Res., *56,* 905–936.

Andersson, M. G. I. 2007. Nitrogen cycling in a turbid, tidal estuary, Ph.D. Thesis, Univ. of Utrecht.

Banta, G. T., M. Holmer, M. H. Jensen and E. Kristensen. 1999. Effects of two polychaete worms, *Nereis diversicolor* and *Arenicola marina,* on aerobic and anaerobic decomposition in a sandy marine sediment. Aquat. Microb. Ecol., *19,* 189–204.

Cardenas, B. and J. L. Wilson. 2006. Hydrodynamics of coupled flow above and below a sediment-water interface with triangular bedforms. Adv. Wat. Res., *30,* 301–313.

Cook, P. L. M., F. Wenzhŀofer, S. Rysgaard, O. S. Galaktionow, F. J. R. Meysman, B. D. Eyre, J. Cornwell, M. Huettel and R. N. Glud. 2006. Quantification of denitrification in permeable sediments: Insights from a two-dimensional simulation analysis and experimental data. Limnol. Oceanogr. Methods., *4,* 294–307.

D'Andrea, A. F., R. C. Aller, and G. R. Lopez. 2002. Organic mater flux and reactivity on a South Carolina sandflat: The impacts of pore water advection and macrobiological structures. Limnol. Oceanogr., *47,* 1056–1070.

De Beer, D., F. Wenzhöfer, T. G. Ferdelman, S. E. Boehme, and M. Huettel. 2005. Transport and mineralization rates in North Sea sandy intertidal sediments, Sylt-Rømø Basin, Wadden Sea. Limnol. Oceanogr., *50,* 113–127.

Engström, P., T. Dalsgaard, S. Helth and R. C. Aller. 2005. Anaerobic ammonium oxidation by nitrite (anammox): Implications for N_2 production in coastal marine sediments. Geochim. Cosmochim. Acta., *69,* 2057–2065.

Emery, K. O. 1966. Atlantic continental shelf and slope of the United States, a geologic background: U.S. Geological Survey Prof., Paper 529-A.

Forster, S. and G. Graf. 1992. Continuously measured changes in redox potential influenced by oxygen penetrating from burrows of Callianassa subterranea. Hydrobiol., *235/236,* 527–532.

—— 1995. Impact of irrigation on oxygen flux into the sediment: intermittent pumping by *Callianassa subterranea* and "piston-pumping" by *Lanice conchilega.* Mar. Biol., *123,* 335–346.

Franke, U., L. Polerecky, E. Precht and M. Huettel. 2006. Wave tank study of particulate organic matter degradation in permeable sediments. Limnol. Oceanogr., *51,* 1084–1096.

Gilbert, F., R. C. Aller and S. Hulth. 2003. The influence of macrofaunal burrow spacing and diffusive scaling on sedimentary nitrification and denitrification: An experimental simulation and model approach. J. Mar. Res., *61,* 101–125.

Glud, R. N., S. Forster and M. Huettel. 1996. Influence of radial pressure gradients on solute exchange in stirred benthic chambers. Mar. Ecol. Prog. Ser., *141,* 303–311.

Hall, P. and R. C. Aller. 1992. Rapid, small-volume, flow injection analysis for ΣCO_2 and NH_4^+ in marine and freshwaters. Limnol. Oceanogr., *37,* 1113–1119.

Hansen, K. and E. Kristensen. 1997. Impact of macrofaunal recolonization on benthic metabolism and nutrient fluxes in a shallow marine sediment previously overgrown with macroalgal mats. Estuar. Coast. Mar. Sci., *45,* 613–628.

Henriksen, K. and M. Kemp. 1988. Nitrification in estuarine and coastal sediments, *in* Nitrogen Cycling in Coastal and Marine Sediments, T. H. Blackburn and J. Sørensen, eds., John Wiley & Sons, New York.

Huettel, M. 1990. Influence of the lugworm *Arenicola marina* on porewater nutrient profiles of sand flat sediments. Mar. Ecol. Prog. Ser., *62,* 241–248.

Huettel, M. and G. Gust. 1992. Impact of bioroughness on interfacial solute exchange in permeable sediments. Mar. Ecol. Prog. Ser., *89,* 253–267.

Huettel, M., W. Ziebis, and S. Forster. 1996. Flow-induced uptake of particulate matter in permeable sediments. Limnol. Oceanogr., *41,* 309–322.

Janssen, F., M. Huettel and U. Witte. 2005. Pore-water advection and solute fluxes in permeable marine sediments (II): Benthic respiration at three sandy sites with different permeabilities (German Bight, North Sea). Limnol. Oceanogr., *50,* 779–792.

Jensen, K. M., M. H. Jensen and E. Kristensen. 1996. Nitrification and denitrification in Wadden Sea sediments (Königshafen, Island of Sylt, Germany) as measured by nitrogen isotope pairing and isotope dilution. Aquat. Micob. Ecol., *11,* 181–191.

Kana, T. M., C. Darkangelo, M. D. Hunt, J. B. Oldham, G. E. Bennett and J. C. Cornwell. 1994. Membrane Inlet Mass Spectrometer for rapid high precision-determination of N_2, O_2 and Ar in environmental water samples. Anal. Chemi., *66,* 4166–4170.

Karlson, K., S. Hulth, K. Ringdahl and R. Rosenberg. 2005. Experimental recolonisation of Baltic Sea reduced sediments: survival of benthic macrofauna and effects on nutrient cycling. Mar. Ecol. Prog. Ser., *294,* 35–49.

Kelly-Gerreyn, B. A., M. Trimmer and D. J. Hydes. 2001. A diagenetic model discriminating denitrification and dissimilatory nitrate reduction to ammonium in a temperate estuarine sediment. Mar. Ecol. Pro. Ser., *220,* 33–46

Kristensen, E. 2001. Impact of polychaetes (*Nereis* spp. and *Arenicola marina*) on carbon biogeo-chemistry in coastal marine sediments. Geochem. Trans., *2*, 92–103.

Kristensen, E., M. H. Jensen and R. C. Aller. 1991. Direct measurement of dissolved inorganic nitrogen exchange and denitrification in individual polychaete (*Neris virens*) burrows. J. Mar. Res., *49*, 355–377.

Marinelli, R, L. 1994. Effects of burrow ventilation on activities of a terebellid polychaete and silicate removal from sediment pore waters. Limnol. Oceanogr., *39*, 303–317.

Marinelli, R. L., C. R. Lovell, S. G. Wakeham, D. B. Ringelberg and D. C. White. 2002. Experimental investigation of the control of bacterial community composition in macrofaunal burrows. Mar. Ecol. Prog. Ser., *235*, 1–13.

Meile, C. and P. Van Cappellen. 2003. Global estimates of enhanced solute transport in marine sediments. Limnol. Oceanogr., *48*, 777–786.

Mermillod-Blondin, F., R. Rosenberg, F. François, K. Norling and L. Mauclaire. 2004. Influence of bioturbation by three benthic species on microbial communities and biogeochemical processes in marine sediment. Aquat. Microb. Ecol., *36*, 271–284.

Meysman, F. J. R., J. J. Middelburg, P. M. J. Herman and C. H. R. Heip. 2003. Reactive transport in surface sediments. II. Media: an object-oriented problem-solving environment for early diagenesis. Comp. Geosci., *29*, 301–318.

Meysman, F. J. R., O. S. Galaktionov and J. J. Middelburg. 2005. Irrigation patterns in permeable sediments induced by burrow ventilation: a case study of *Arenicola marina.* Mar. Ecol. Prog. Ser., *303*, 195–212.

Meysman, F. J. R., O. S. Galaktionov, B. Gribsholt, and J. J. Middelburg. 2006. Bio-irrigation in permeable sediment: Advective pore water transport induced by burrow ventilation. Limnol. Oceanogr., *51*, 142–156.

Meysman, F. J. R., O. S. Galaktionov, P. L. M. Cook, F. Janssen, M. Huettel, and J. J. Middelburg. 2007. Quantifying biologically and physically induced flow and tracer dynamics in permeable sediments. Biogeosciences., *4*, 627–646.

Nieuwenhuize, J., Y. E. M. Maas and J. J. Middelburg. 1994. Rapid analysis of organic-carbon and nitrogen in particulate materials. Mar. Chem., *45*, 217–224.

Nielsen, L. P. 1992. Denitrification in sediments determined from nitrogen isotope paring. FEMS Microbiol. Ecol., *86*, 357–362.

Papaspyrou, S., E. Kristensen and B. Christensen. 2007. *Arenicola marina* (Polychaeta) and organic matter mineralization in sandy marine sediments: *In situ* and microcosm comparison. Estuar. Coast. Mar. Sci., *72*, 213–222.

Parson, T. R., Y. Maita and C. M. Lalli. 1984. A manual of chemical and biological methods for seawater analysis. Pergamon. Oxford.

Pelegri, S. P. and T. H. Blackburn. 1994. Bioturbation effects of the amphipod *Corophium volutator* on microbial nitrogen transformations in marine sediments. Mar. Biol., *121*, 253–258.

Precht, E. and M. Huettel. 2003. Advective pore-water exchange driven by surface gravity waves and its ecological implications. Limnol. Oceanogr., *48*, 1674–1684.

Raine, R. C. T. and J. W. Patching. 1980. Aspects of carbon and nitrogen cycling in a shallow marine environment. J. Exp. Mar. Biol. Ecol., *47*, 127–139.

Rao, A. M. F., M. J. McCarthy, W. S. Gardner and R. A. Jahnke. 2007. Respiration and denitrification in permeable continental shelf deposits on the South Atlantic Bight: Rates of carbon and nitrogen cycling from sediment column experiments. Cont. Shelf Res., *27*, 1801–1891.

Rao, A. M. F., M. J. McCarthy, W. S. Gardner, and R. A. Jahnke. 2008. Respiration and denitrification in permeable continental shelf deposits on the South Atlantic Bight: N2:Ar and isotope pairing measurements in sediment column experiments. Cont. Shelf Res., *28*, 602–613.

Reichardt, W. 1988. Impact of the Antarctic benthic fauna on the enrichment of biopolymer degrading psychrophilc bacteria. Microb. Ecol., *15,* 311–321.

Reimers, C. E., III H. A. Stecher, G. L. Taghon, C. M. Fuller, M. Huettel, A. Rusch, N. Ryckelynck and C. Wild. 2004. *In situ* measurements of advective solute transport in permeable shelf sands. Continent. Shelf. Res. *24,* 183–201.

Rhoads, D. C. 1974. Organism-sediment relations on the muddy sea floor. Oceanogr. Mar. Biol. Ann. Rev., *12,* 223–300.

Riedl, R. J., N. Huang and R. Machan. 1972. The subtidal pump: a mechanism of interstitial water exchange by wave action. Mar. Biol., *13,* 210–221.

Riisgård, H. U., I. Berntsen and B. Tarp. 1996. The lugworm (*Arenicola marina*) pump: characteristics, modelling and energy cost. Mar. Ecol. Prog. Ser., *138,* 149–156.

Riisgård, H. U. and G. T. Banta. 1998. Irrigation and deposit feeding by the lugworm *Arenicola marina,* characteristics and secondary effects on the environment: A review of current knowledge. Vie Milieu., *48,* 243–257.

Shum, K. T. and B. Sundby. 1996. Organic matter processing in continental shelf sediments—the subtidal pump revisited. Mar. Chem., *53,* 81–87.

Tang, M. and E. Kristensen. 2007. Impact of microphytobenthos and macroinfauna on temporal variation of benthic metabolism in shallow coastal sediments. J. Exp. Mar. Biol. Ecol., *349,* 99–112.

Thibodeaux, L. J. and J. D. Boyle. 1987. Bedform-generated convective-transport in bottom sediment. Nature, *325,* 341–343.

Timmermann, K., G. T. Banta and R. N. Glud. 2006. Linking *Arenicola marina* irrigation behavior to oxygen transport and dynamics in sandy sediments. J. Mar. Res., *64,* 915–938.

Vopel, K., D. Thistle and R. Rosenberg. 2003. Effect of the brittle star *Amphiura filiformis* (Amphiuridae, Echinodermata) on oxygen flux into the sediment. Limnol. Oceanogr., *48,* 2034–2045.

Wang, Y. E. and P. Van Cappellan. 1996. A multicomponent reactive transport model of early diagenesis: application to redox cycling in coastal marine sediments. Geochim. Cosmochim. Acta., *60,* 2993–3014.

Waldbusser, G. G. and R. L. Marinelli. 2006. Macrofaunal modification of porewater advection: role of species function, species interaction, and kinetics. Mar. Ecol. Prog. Ser., *311,* 217–231.

Webb, A. P. and B. D. Eyre. 2004. Effect of natural populations of burrowing Thalassinidean shrimp on sediment irrigation, benthic metabolism, nutrient fluxes and denitrification. Mar. Ecol. Prog. Ser., *268,* 205–220.

Wenzhöfer, F. and R. N. Glud. 2004. Small-scale spatial and temporal variability in coastal benthic O2 dynamics: Effects of fauna activity. Limnol. Oceanogr., *49,* 1471–1481.

Wethey, D. S. and S. A. Woodin. 2005. Infaunal hyraulics generate porewater pressure signals. Biol. Bull., *209,* 139–145.

Wethey, D. S., S. A. Woodin, N. Volkenborn and K. Reise. 2008. Porewater advection by hydraulic activities of lugworms, *Arenicola marina*: A field, laboratory and modeling study. J. Mar. Res., *66,* 255–273.

Zebe, E. and D. Schiedeck. 1996. The lugworm *Arenicola marina*: a model of physiological adaptation to life in intertidal sediments. Helgoländer Meersuntersuchungen. *50,* 37–68.

Ziebis, W., S. Forster, M. Huettel and B. B. Jorgensen. 1996. Complex burrows of the mud shrimp *Callianassa Truncata* and their geochemical impact in the sea bed. Nature, *382,* 619–622.